

Precision extraction of a_{nn} from $\pi^- d \rightarrow nn\gamma$ using chiral perturbation theory

A. Gårdestig

Department of Physics and Astronomy
 University of South Carolina
 Columbia, SC 29208
 U. S. A.

D. R. Phillips

Department of Physics and Astronomy
 Ohio University
 Athens, OH 45701
 U. S. A.

Abstract

The neutron-neutron scattering length a_{nn} provides a sensitive probe of charge-symmetry breaking in the strong interaction. Here we summarize our recent efforts to use chiral perturbation theory in order to systematically relate a_{nn} to the shape of the neutron spectrum in the reaction $\pi^- d \rightarrow nn\gamma$. In particular we show how the chiral symmetry of QCD relates this process to low-energy electroweak reactions such as $pp \rightarrow de^+\nu_e$. This allows us to reduce the uncertainty in the extracted a_{nn} (mainly due to short-distance physics in the two-nucleon system) by a factor of more than three, to < 0.05 fm. We also report first results on the impact that two-nucleon mechanisms of chiral order P^4 have on the $\pi^- d \rightarrow nn\gamma$ neutron spectrum.

1 Introduction

Quantum chromodynamics (QCD) is almost symmetric under the interchange of the up and down quarks. This is called charge symmetry, and is due to the fact that the mass difference $m_d - m_u$ is much smaller than the QCD mass scale $\Lambda \sim 1$ GeV. This symmetry, which is a subgroup of isospin symmetry $SU(2)_V$, is well-respected in strong interactions at low energies, but is softly broken by quark-mass differences, and also by electromagnetic effects. The

relevant dimensionless parameters governing charge-symmetry breaking are therefore $\frac{m_d - m_u}{\Lambda}$ and $\frac{\alpha_{em}}{\pi}$, both of which are less than 1%. Although it is indeed generally of this small magnitude, charge-symmetry breaking (CSB) has many experimentally verifiable effects in hadronic and nuclear physics, such as the neutron-proton mass difference, rho-omega mixing, the binding-energy difference of mirror nuclei (e.g., ${}^3\text{He}$ and ${}^3\text{H}$), the recently measured forward-backward symmetry for $np \rightarrow d\pi^0$ [1], and the $dd \rightarrow \alpha\pi^0$ reaction [2]. For comprehensive reviews of charge symmetry and its breaking see Ref. [3].

The difference between the strong-interaction parts of the nn and pp scattering lengths ($a_{pp}^{\text{str}} - a_{nn}^{\text{str}}$) is particularly sensitive to CSB. The scattering length parameterizes the zero-energy NN scattering phase shift, $\delta(p)$, via:

$$a \equiv -\lim_{p \rightarrow 0} \frac{\delta(p)}{p}, \quad (1)$$

where p is the NN relative momentum. Hence the (strong) nn and pp scattering lengths would be equal in the limit of exact charge symmetry. Their difference is an important quantity for two, somewhat related reasons. Firstly, the nucleon-nucleon scattering lengths are unnaturally large compared to the pion Compton wavelength. This is indicative of fine tuning in the NN potential and in consequence the CSB piece of the NN potential has an impact on the scattering lengths that is greatly enhanced [3]:

$$\frac{a_{pp}^{\text{str}} - a_{nn}^{\text{str}}}{a} = (10 - 15) \frac{\Delta V_{\text{CSB}}}{V_{NN}}. \quad (2)$$

Measurements of $a_{pp} - a_{nn}$ therefore provide significant constraints on CSB terms in modern phenomenological NN potentials, e.g., AV18 [4]. Secondly, when potentials fit to the currently accepted values $a_{nn} = -18.59 \pm 0.4$ fm and $a_{pp} = -17.3 \pm 0.4$ fm [5] are used to make predictions for binding energies of mirror nuclei, they very accurately reproduce the experimental binding-energy difference of, e.g., the aforementioned ${}^3\text{H}$ and ${}^3\text{He}$ [6].

Both a_{nn} and a_{pp} must have electromagnetic corrections applied to them in order to extract the strong-interaction part. This correction is huge for the pp case, but is under good theoretical control. In the nn case the electromagnetic correction is due to a magnetic-moment interaction and is ≈ -0.3 fm.

But on the nn side there is an experimental difficulty in obtaining dense enough free nucleon targets. There have been some attempts at doing direct nn measurements, the most recent one being pursued at the pulsed reactor YAGUAR [7]. However, the more promising approaches so far have been based on indirect measurements, where final-state neutrons are detected in regions of phase space where they have low relative energy and hence observables are sensitive to the nn scattering length.

Unfortunately, the two most recent measurements employing the $nd \rightarrow nnp$ reaction for this purpose extract very different a_{nn} values. Thus, a Bonn group reported $a_{nn} = -16.1 \pm 0.4$ fm [8], while a group based at TUNL claimed $a_{nn} = -18.7 \pm 0.7$ fm [9], a 4σ disagreement.

However, experiments at different facilities based on the alternative process $\pi^-d \rightarrow nn\gamma$ [10,11], have yielded consistent values for many years. Thus these results dominate the “accepted” value of a_{nn} quoted above. The scattering length is extracted by fitting the shape of the spectrum of neutrons emitted from the decay of the pionic deuterium atom. The theoretical uncertainty in the a_{nn} extracted using extant calculations [12,13] is $\approx \pm 0.3$ fm, dominated by the uncertainties in the nn wave function at short distances.

In the present work we revisit these calculations for radiative pion capture on deuterium and take advantage of the modern development of effective field theory (EFT), in particular chiral perturbation theory (χ PT). By using an EFT we have consistency between the wave functions and production/capture amplitudes, a recipe to estimate the theoretical error, and we can make systematic improvements when necessary. Also, in the case of χ PT, we gain a close connection to the underlying theory QCD through QCD’s chiral symmetry. In the next section we describe the key elements of our χ PT calculation of $\pi^-d \rightarrow nn\gamma$, and in Section 3 we present the results already obtained in recent publications [14–16], and also provide a first report on substantial improvements of these calculations.

2 Anatomy of the Calculation

EFTs circumvent the problem of the large QCD coupling constant at low energies. Instead one expands amplitudes in the ratio P/Λ , where $P \sim m_\pi$ is a small energy/momentum of the problem and $\Lambda \sim 1$ GeV is the scale of chiral-symmetry breaking. This power counting provides a hierarchy of quantum-mechanical amplitudes which allows for an systematic organization of the calculation. (We count the electron charge e as one power of P/Λ .)

In the application of chiral perturbation theory to nuclear processes, classes of graphs must be resummed in order to generate the nuclear bound states observed in nature. The original proposal for such resummation is due to Weinberg [17]. Applying it to the case at hand we see that the amplitude for $\pi^-d \rightarrow nn\gamma$ should be calculated as:

$$\mathcal{A} = \langle \mathbf{p} | \hat{O} | \psi_d \rangle + \langle \mathbf{p} | T_{nn} G_0 \hat{O} | \psi_d \rangle, \quad (3)$$

where $|\psi_d\rangle$ is the deuteron wave function (which is dominated by modes with momenta where χ PT is applicable), $|\mathbf{p}\rangle$ is a plane wave with the observed rel-

ative momentum of the two final-state neutrons, \mathbf{p} , T_{nn} is the nn rescattering amplitude, and G_0 the free nn Green function.

Meanwhile \hat{O} is the operator (technically the two-particle irreducible kernel) governing the transition $\pi^- np \rightarrow nn\gamma$. Weinberg proposed that \hat{O} has a well-behaved chiral expansion and so can be calculated in χ PT. (For a summary of the successful application of this idea to electromagnetic processes see Ref. [18].) \hat{O} has one- and two-body pieces, with the one-body part in this case beginning at $\mathcal{O}(P)$ with the Kroll-Ruderman term for $\pi^- p \rightarrow n\gamma$. Two-body pieces enter at $\mathcal{O}(P^3)$. In this work we report on calculations obtained from a partial $\mathcal{O}(P^4)$ (next-to-next-to-next-leading order = N3LO) calculation of \hat{O} . Our calculation includes all mechanisms at $\mathcal{O}(P^3)$ (N2LO), but only the dominant $\mathcal{O}(P^4)$ two-body pieces of \hat{O} .

2.1 Chirally inspired wave functions

In order to reach the desired accuracy in the calculation of \mathcal{A} , the NN wave functions have to be calculated to an order that is consistent with that to which \hat{O} is obtained. Here this means that they must be computed up to $\mathcal{O}(P^3)$ and thus include the leading- and sub-leading two-pion-exchange corrections to the chiral NN potential [19]. The necessary deuteron and nn scattering wave functions are derived starting from the asymptotic states, given by the asymptotic normalization A_S and D/S ratio for the deuteron and the effective-range expansion for nn scattering. These are integrated in from $r = \infty$ using the Schrödinger equation with the chiral one- and two-pion exchange potentials. Eventually, we reach a region, at $r = 1\text{--}2$ fm, where the chiral expansion for the NN potential breaks down. We take the simple approach of introducing a cutoff R in this range and assume that the potential for $r < R$ is given by a square well whose depth we adjust to enforce continuity of the wave function at $r = R$. This parameterizes and regularizes our ignorance of the short-distance NN physics. It is then important to ensure that the result is independent of the cutoff R to the order we are working, i.e., that the renormalization-group criteria are fulfilled.

2.2 One-body amplitudes to NNLO

The chiral one-body amplitudes have been calculated by Fearing *et al.* [20] up to $\mathcal{O}(P^3)$, fitting the available $\gamma p \rightarrow \pi^+ n$ and $\pi^- p \rightarrow \gamma n$ data via the adjustment of χ PT low-energy constants (LECs). A preliminary estimate of the size of the N3LO one-body amplitude indicates that it has negligible influence on $\pi^- d \rightarrow nn\gamma$ and hence we do not discuss it further here [21].

2.3 Two-body amplitudes to N3LO

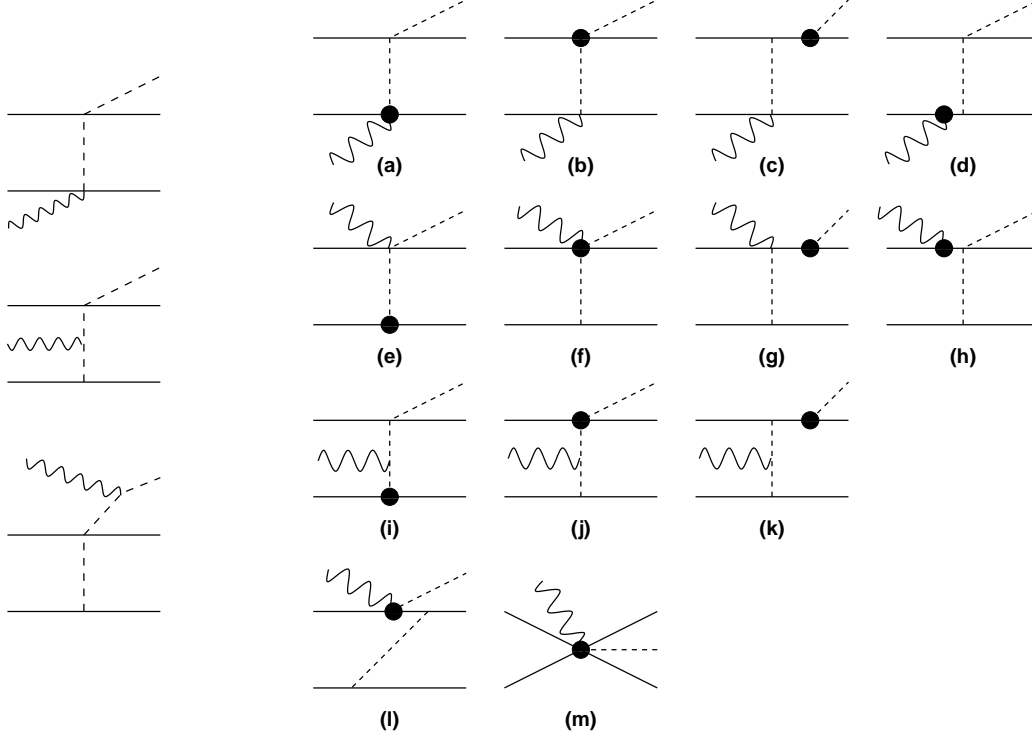


Figure 1: The two-body diagrams relevant for $\pi^- d \rightarrow nn\gamma$. Left: $\mathcal{O}(P^3)$. Right: $\mathcal{O}(P^4)$. Only one representative vertex ordering is given for each type of diagram. The black discs indicates insertions from $\mathcal{L}_{\pi N + \pi NN}^{(2)}$.

At $\mathcal{O}(P^3)$ (N2LO), there are the three diagrams given to the left in Fig. 1. The first is believed to be larger than the second since the pion mass disappears from its single propagator and the pion can go on-shell, while the second has, in addition, also one off-shell propagator. The third diagram vanishes in Coulomb gauge. At N3LO [$\mathcal{O}(P^4)$], a slew of diagrams appear, given to the right in Fig. 1 and discussed in detail in [16]. The overall result for the neutron time-of-flight spectrum when all these graphs except for (l) are included is depicted in Fig. 3. Diagram (l) is related to the orthonormalization of the wave functions. Since this is suppressed by $1/M$, we expect that effects due to c_2 – c_4 , which appear in the two-body currents computed in Ref. [16] that are included in our calculation, will be substantially larger. A complete calculation of the $\mathcal{O}(P^4)$ correction, including orthonormalization, is under way [21].

2.4 Constraining unknown short-distance physics

Fig. 3 shows that the neutron spectrum calculated at $\mathcal{O}(P^4)$ with different values of the regulator radius R and a fixed value of the short-distance coefficient in diagram (m) is significantly different in the final-state-interaction (FSI) region. Since a_{nn} is extracted by fitting the shape of the spectrum in the FSI region [11] this sensitivity to unconstrained physics of the NN system seems to limit the accuracy with which a_{nn} can be obtained from $\pi^- d \rightarrow nn\gamma$. We now show how to remedy this problem.

The LO contribution to the matrix element in this region is given by

$$\mathcal{M}_{FSI} \equiv C \int_0^\infty dr u_{nn}(r; p) j_0\left(\frac{kr}{2}\right) u_d(r), \quad (4)$$

where k is the momentum of the outgoing photon, C is a constant that is fixed by e , g_A , f_π , etc., j_0 is the spherical Bessel function of zeroth order, and $u_d [u_{nn}(r; p)]$ is the radial S-wave wave function of the deuteron (1S_0) state. But the short-distance part of this matrix element is the same as that of the pp fusion matrix element

$$\mathcal{M}_{GT} \equiv \int_0^\infty dr u_{pp}(r) u_d(r). \quad (5)$$

This connection is shown empirically in Fig. 2, revealing a linear relationship between the Gamow-Teller matrix element \mathcal{M}_{GT} , and the FSI peak height in $\pi^- d \rightarrow nn\gamma$, $\Gamma_{FSI} \sim |\mathcal{M}_{FSI}|^2$.

This can be understood from the structure of the chiral Lagrangian. It contains both one-nucleon and two-nucleon terms linear in the axial field u_μ :

$$\begin{aligned} \mathcal{L} = & N^\dagger (i v \cdot D + g_A S \cdot u) N \\ & - 2d_1 N^\dagger S \cdot u N N^\dagger N + 2d_2 \epsilon^{abc} \epsilon_{\kappa\lambda\mu\nu} v^\kappa u^{\lambda,a} N^\dagger S^\mu \tau^b N N^\dagger S^\nu \tau^c N \dots, \end{aligned} \quad (6)$$

where

$$f_\pi u_\mu = -\tau^a \partial_\mu \pi^a - \epsilon^{3ba} V_\mu \pi^b \tau^a + f_\pi A_\mu + \mathcal{O}(\pi^3), \quad (7)$$

V_μ (A_μ) is an external vector (axial) field, and the $d_i = \mathcal{O}(\frac{1}{Mf_\pi^2})$ are (a priori unknown) LECs. Since u_μ contains the pion pseudovector coupling, as well as a pion-photon coupling and the axial field A_μ , this is the chiral explanation behind the well-known Goldberger-Treiman (GT) relation and Kroll-Ruderman (KR) terms. In the two-nucleon sector, the same features of u_μ imply a connection between pion p -wave production, pion photoproduction on the NN system, and axial currents—two-body analogs of the GT and KR. The connection between pion production and electroweak processes is currently being investigated by Nakamura [22].

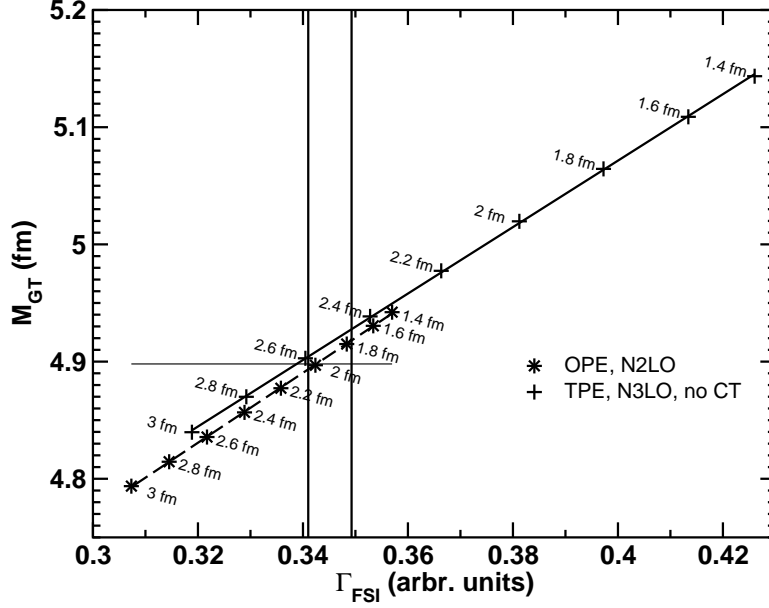


Figure 2: Gamow-Teller matrix element plotted against $\pi^- d \rightarrow nn\gamma$ FSI peak height for various values of R and at different orders and wave functions. The points correspond to the values of R (in fm) indicated. The straight lines are linear fits to the points. The vertical lines show the range in Γ_{FSI} after renormalization, given the M_{GT} value indicated by the horizontal line.

For Gamow-Teller ($^1S_0 \leftrightarrow ^3S_1$) transitions, the LECs only appear in the combination

$$\hat{d} \equiv \hat{d}_1 + 2\hat{d}_2 + \frac{\hat{c}_3}{3} + \frac{2\hat{c}_4}{3} + \frac{1}{6}, \quad (8)$$

where $g_A \hat{d}_i \equiv M f_\pi^2 d_i$ and $\hat{c}_i \equiv M c_i$ [23]. This LEC also appears in p -wave pion production in NN collisions, tritium β decay, pp fusion, νd scattering, $\mu^- d \rightarrow nn\nu_\mu$, and the hep reaction. In addition, if the emitted pion couples to a third nucleon, this same operator and coefficient enters the leading chiral three-nucleon force. These and other implications are discussed further in Refs. [15, 16]. The key point in the context of this work is that chiral symmetry and gauge invariance together explain the linear correlation between pp fusion and the FSI peak height that is evident in Fig. 2.

Now, the solar pp fusion process has recently been calculated very accurately by constraining its unknown short-distance physics from precise calculations of tritium beta decay [23]. If we adjust the LEC that appears in diagram (m) to reproduce this rate for $pp \rightarrow de^+\nu_e$ we obtain a very precise prediction for the FSI peak height in $\pi^- d \rightarrow nn\gamma$, as shown in Fig. 2.

3 Results

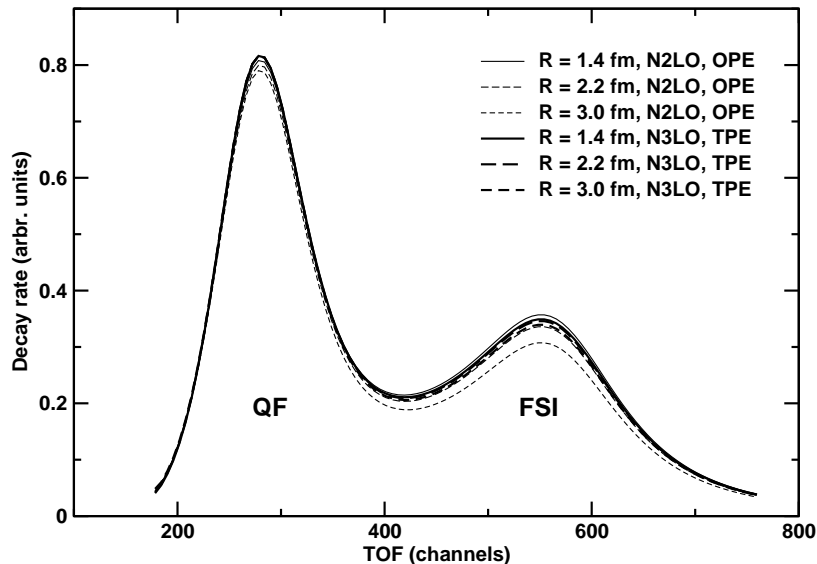


Figure 3: The neutron time-of-flight spectrum for $\pi^- d \rightarrow nn\gamma$ at different cutoffs R and orders as indicated. The thin lines are for the N3LO calculation with wave functions calculated with the chiral one-pion exchange potential, while the thick lines include N3LO two-body currents and the chiral two-pion exchange potential as well. The latter coincide at the quasi-free (QF) peak and show a much reduced spread in the FSI peak.

The result of this renormalization can be seen in Fig. 3. Clearly the N3LO contribution reduces the cutoff dependence considerably compared to N2LO. The theoretical uncertainty due to unknown short-distance physics in the NN system is now negligible in the FSI region. A detailed analysis of the other theoretical uncertainties (see Ref. [14]) reveals that the total theoretical error in the extracted a_{nn} at N3LO is ± 0.3 fm when the entire spectrum is fitted and ± 0.05 fm if only the FSI peak is fitted.

4 Conclusions

Chiral perturbation theory relates the unknown short-distance physics of various electroweak two-body observables to pion p -wave production and pion photoproduction on two nucleons. (We can also constrain a piece of the chiral three-nucleon force from electroweak two-body observables.) This connection

makes it possible to calculate $\pi^-d \rightarrow nn\gamma$ to high precision, leading to a small theoretical error for the extraction of a_{nn} : $\Delta a_{nn}^{\text{theory}} = \pm 0.05$ fm. This reduces that error by at least a factor of three compared to previous calculations.

A future publication [21] will contain a full description of the amplitudes and wave functions employed in our N3LO calculation. In that work we will also investigate the influence of higher-order electromagnetic corrections in the pp wave functions used for $pp \rightarrow de^+\nu_e$ and whether we are justified in neglecting the N3LO one-body contribution. We also provide a full accounting of the $1/M$ corrections to the two-body operators that are mandated by the unitary transformations used to obtain a Hermitian NN potential V .

In addition we are investigating the possibility to constrain \hat{d} directly from a two-body observable by calculating the $\mu^-d \rightarrow nn\nu_\mu$ capture rate in the same framework [24]. This reaction is soon to be measured at the Paul Scherrer Institute to 1% precision [25]. It would also be interesting to revisit the neutrino-deuteron breakup reactions that are important for the SNO detector. Another possible direction would be to complete the circle by calculating tritium beta decay using chiral three-nucleon wave functions with the r -space regularization we have used in the NN sector.

Acknowledgments

This work was supported by the Institute for Nuclear and Particle Physics at Ohio University, by DOE grant DE-FG02-93ER40756, and by NSF grant PHY-0457014.

References

- [1] A. K. Oppen *et al.*, *Phys. Rev. Lett.* **91**, 212302 (2003).
- [2] E. J. Stephenson *et al.*, *Phys. Rev. Lett.* **91**, 142302 (2003).
- [3] G. A. Miller, B. M. K. Nefkens, and I. Šlaus, *Phys. Rep.* **194**, 1 (1990);
G. A. Miller and W. van Oers, arXiv:nucl-th/9409013; G. A. Miller, A. Oppen, and E. J. Stephenson, *Ann. Rev. Nucl. Part. Sci.* **56**, 293 (2006).
- [4] R. B. Wiringa, V. G. J. Stoks, and R. Schiavilla, *Phys. Rev. C* **51**, 38 (1995).
- [5] R. Machleidt and I. Šlaus, *J. Phys. G* **27**, R69 (2001).
- [6] S. C. Pieper and R. B. Wiringa, *Annu. Rev. Nucl. Part. Sci.* **51**, 53 (2001).

- [7] W. I. Furman *et al.*, *J. Phys. G: Nucl. Part. Phys.* **28**, 2627 (2002).
- [8] V. Huhn *et al.*, *Phys. Rev. Lett.* **85**, 1190 (2000).
- [9] D. E. González Trotter *et al.*, *Phys. Rev. Lett.* **83**, 3788 (1999). *Phys. Rev. C* **73**, 034001 (2006).
- [10] B. Gabioud *et al.*, *Phys. Rev. Lett.* **42**, 1508 (1979); *Phys. Lett.* **103B**, 9 (1981); *Nucl. Phys.* **A420**, 496 (1984); O. Schori *et al.*, *Phys. Rev. C* **35**, 2252 (1987).
- [11] C. R. Howell *et al.*, *Phys. Lett. B* **444**, 252 (1998).
- [12] W. R. Gibbs, B. F. Gibson, and G. J. Stephenson, Jr., *Phys. Rev. C* **11**, 90 (1975); **16**, 322 (1977); **16**, 327 (1977).
- [13] G. F. de Téramond, *Phys. Rev. C* **16**, 1976 (1977); G. F. de Téramond, J. Páez, and C. W. Soto Vargas, *ibid.* **21**, 2542 (1980); G. F. de Téramond and B. Gabioud, *ibid.* **36**, 691 (1987).
- [14] A. Gårdestig and D. R. Phillips, *Phys. Rev. C* **73**, 014002 (2006).
- [15] A. Gårdestig and D. R. Phillips, *Phys. Rev. Lett.* **96**, 232301 (2006).
- [16] A. Gårdestig, *Phys. Rev. C* **74**, 017001 (2006).
- [17] S. Weinberg, *Nucl. Phys. B* **363**, 3 (1991); *Phys. Lett. B* **251**, 288 (1990).
- [18] D. R. Phillips, these proceedings.
- [19] C. Ordonéz, L. Ray, and U. van Kolck, *Phys. Rev. C* **53**, 2086 (1996); N. Kaiser, R. Brockmann, and W. Weise, *Nucl. Phys.* **A625**, 758 (1997); E. Epelbaum, W. Glöckle, and U.-G. Meißner, *Nucl. Phys.* **A671**, 295 (1999); M. C. M. Rentmeester, *et al.*, *Phys. Rev. Lett.* **82**, 4992 (1999).
- [20] H. W. Fearing *et al.*, *Phys. Rev. C* **62**, 054006 (2000).
- [21] A. Gårdestig and D. R. Phillips, (in preparation).
- [22] S. X. Nakamura, arXiv:0709.1239 [nucl-th] and these proceedings.
- [23] T.-S. Park *et al.*, *Phys. Rev. C* **67**, 055206 (2003).
- [24] A. Gårdestig, T.-S. Park, K. Kubodera, and F. Myhrer, (in preparation).
- [25] P. Kammel, talk at *International Conference on Muon Catalyzed Fusion and Related Topics*, Dubna, Russia (2007).